Ice stream activity scaled to ice sheet volume during Laurentide Ice Sheet deglaciation

C. R. Stokes[1], M. Margold[1†], C.D. Clark[2], L. Tarasov[3]

[1]*Department of Geography, Durham University, Durham, UK*

[2]*Department of Geography, University of Sheffield, Sheffield, UK*

[3]*Department of Physics and Physical Oceanography, Memorial University, St John's, Canada*

**Correspondence to: c.r.stokes@durham.ac.uk*

[†]*Present address: Department of Physical Geography, Stockholm University, Sweden*

The sea-level contribution of the Greenland and West Antarctic ice sheets has accelerated in recent decades, largely due to the thinning and retreat of outlet glaciers and ice streams[1-4]. This 'dynamic' loss is a serious concern, with some modelling studies suggesting that a major ice sheet collapse may be imminent[5,6] or potentially underway in West Antarctica[7], but others predicting a more limited response[8]. A major problem is that observations used to initialise and calibrate modelling typically span just a few decades and, at the ice-sheet scale, it is unclear how the entire drainage network of ice streams evolves over longer time-scales. This represents one of the largest sources of uncertainty when predicting ice sheet contributions to sea level rise[8-10]. A key question is whether ice streams might increase and sustain rates of mass loss over centuries or millennia, beyond those expected for a given ocean-climate forcing[5-10]. Here we reconstruct the activity of 117 ice streams that operated at various times during deglaciation of the Laurentide Ice Sheet (~22,000 to ~7,000 years ago) and show that while they switched on and off in different locations, their overall number decreased,

they occupied a progressively smaller percentage of the ice sheet perimeter, and their total discharge decreased. Underlying geology and topography clearly influenced ice stream activity, but - at the ice sheet scale - their drainage network adjusted and was linked to changes in ice sheet volume. It is unclear whether these findings are directly translatable to modern ice sheets but, contrary to the view that sees ice streams as unstable entities that can draw-down large sectors of an ice sheet and accelerate its demise, we conclude that they reduced in effectiveness during deglaciation of the Laurentide Ice Sheet.

Continental ice sheets are drained by a network of rapidly-flowing ice streams with tributaries of intermediate velocity that extend far into their interiors[11]. Towards the margins of modern ice sheets, many ice streams become confined within glacial troughs and are referred to as marine-terminating outlet glaciers, whereas others occupy regions of more subdued relief[12]. Their large size (1-10s km wide, 10-100s km long) and high velocity (100s-1000s m a^{-1}) means they are an important mechanism through which ice is transferred to the ocean, and thereby impacts on sea level. In contrast to climatically-forced melting[13], ice-stream dynamics could introduce considerable non-linearity in the response of ice sheets to external forcing[5-7]. This is viewed as the major source of uncertainty in assessments of future changes in ice sheets and sea level[1,6,8-10]. Does the drainage network of ice streams arise in response to climatically-driven changes in ice sheet volume, or can it evolve to drive changes beyond that which might be expected from climatic forcing alone?

Building on a recent inventory[14] of 117 palaeo-ice streams in the North American Laurentide Ice Sheet (LIS, including the Innuitian Ice Sheet, but excluding the Cordilleran Ice Sheet) (Extended Data Figure 1), we use the best-available ice margin chronology (based on ~4,000 dates: Extended Data Figure 2)[15] to ascertain the timing of their activity during deglaciation (see Methods). Using the mapped extent of ice streams, we calculated the

number operating through time and the percentage of the ice sheet perimeter that was streaming. We also explore their potential ice discharge during deglaciation, albeit with larger uncertainties, which we compare with output from numerical modelling of the ice sheet during deglaciation[16,17] (see Methods).

When the LIS was at its maximum extent ~22 thousand years ago (kyr), ice streams formed a drainage network resembling the velocity pattern of modern-day ice sheets (Fig. 1a, b). Early during deglaciation, numerous ice streams were located in major topographic troughs and drained the marine-based sectors of the northern and eastern margins of the ice sheet for several thousand years (Fig. 1b, c). Ice streaming along the land-terminating margins was more transient and we find that numerous ice streams switched on and off in different locations during retreat. This first empirical assessment of the duration of a large population of ice streams reveals that whilst some ice streams persisted for 5-10 kyr, ~40% operated for <2 kyr, with many (~23%) operating for <0.5 kyr (Fig. 2).

Although ice streams activated and deactivated in different locations, we find no evidence for any episodes when the number of ice streams increased substantially (Fig. 3a). From ~22 to ~15.5 kyr, the number of ice streams totalled ~50, but thereafter dropped rapidly (e.g. at ~13 kyr and 11.5 kyr), with <10 ice streams operating after ~11.5 kyr. When normalised by ice sheet volume their number is remarkably stable (Fig. 3b), with ~2 ice streams per 1,000,000 km^3 of ice sheet volume for almost 10 kyr. LIS collapse into Hudson Bay after 8.5 kyr triggered a final flurry of ice stream activity, but in a very small ice sheet.

At its maximum extent, ~27% of the LIS margin was streaming (Fig. 3c), which is very similar to that found for present-day Antarctica (Fig. 1a). This value decreased to between 25% and 20% from 16 to 13 kyr, but then rapidly drops to ~5% at ~11 kyr. Similarly, our order-of-magnitude estimates of palaeo-ice stream discharge show no obvious increases during deglaciation (Fig. 3d). Rather, this ‘dynamic’ component of mass loss was

relatively stable from ~22 to 15 kyr (i.e. ~1,500 km^3 a^{-1}), but then rapidly decreased to <400 km^3 a^{-1} after 11 kyr, and was <100 km^3 a^{-1} after 9 kyr. When normalised by ice sheet volume, the proportion of dynamic mass loss was relatively stable from 22 to 15 kyr, but then dropped at 13 kyr (Fig. 3e), before increasing temporarily as the ice sheet collapsed around Hudson Bay. A comparison with estimates of total ice stream discharge from a previously-published numerical model of the North American Ice Sheet complex[16] and inferences from surface mass balance modelling at specific time-steps[17], indicates that model-derived Laurentide ice stream discharges are typically higher and more variable (Fig. 3f). Nevertheless, an important conclusion is that both empirical and modelled estimates show a decrease in ice stream discharge from around 15 kyr. Moreover, we find a clear link between ice sheet volume and both the number of ice streams and the percentage of the ice sheet perimeter they occupied (Fig. 4a, b). A similar scaling is seen in both modelled and empirically-derived discharge (Fig. 4c), but we acknowledge there are much larger uncertainties in our estimates of palaeo-ice stream discharge. The relative impact of ice streaming is seen more clearly by plotting ice sheet volume against the total ice stream discharge normalised by the ice sheet volume (Fig. 4d), indicating that the relative role of mass loss from streaming was unlikely to have increased as the ice volume decreased during deglaciation.

There are a number of factors that influence where ice streams develop, with previous work highlighting their strong association with topographic troughs, calving margins and soft sedimentary beds[10,18,19]. We note that topography exerted a strong control on ice stream location in the LIS, particularly during early deglaciation (22 to 14 kyr) when its flow was steered by the major marine channels of the Canadian Arctic Archipelago and the high relief coasts along the eastern margin. There is no glacial geomorphological evidence[14] that these ice streams continued to operate once the ice sheet lost its marine margin and retreated onto

lower relief terrain. Thus, topographic troughs and the marine margin clearly modulated the number of ice streams operating through time (Fig. 1; Fig. 3a).

Elsewhere, ice streams were abundant on low-relief areas that were underlain by soft sedimentary bedrock and thick sequences of till. This includes the western and southern margins of the ice sheet[14,19,20], where numerous ice streams switched on and off during deglaciation, with marked changes in trajectory[20] (Fig. 1). These networks of sinuous ice streams deactivated as the ice margin withdrew onto the harder igneous and metamorphic rocks of the Canadian Shield, pointing to a geological control that explains the marked reduction in ice stream numbers after ~12 ka (Fig. 3a; Extended Data Figure 3). It is important to note, however, that ice streams continued to activate over the low-relief crystalline bedrock of the Canadian Shield, with several large, wide (100-200 km) ice streams operating for very short periods (few hundred years) during the final stages of deglaciation (after ~10 kyr: Fig. 1d; Extended Data Fig. 3)[10,21].

Although topography and underlying geology exerted an important influence on ice stream activity, we find no evidence for major ice sheet instabilities linked to ice stream activity that is reflected in the spatial re-organisation of their drainage network (e.g. marked increases in the number of ice streams or individual ice streams widening/enlarging during ice sheet retreat). Rather, we find that their overall number decreased and they occupied a progressively smaller percentage of the ice sheet perimeter. This implies that the final 4-5 kyr of deglaciation (after ~12 kyr) was largely driven by surface melt, which is corroborated by independent modelling of the ice sheet's surface mass balance[17,22], and inferences based on the density of subglacial meltwater channels (eskers)[23]. Specifically, surface energy balance modelling[17] suggests that a transition from a positive to negative surface mass balance occurred between 11.5 and 9 kyr, when much of the LIS retreat occurred at rates two to five times faster than before 11.5 kyr. In that study[17], volume losses not attributable to surface

125 melting were assumed to be from dynamic discharge and, in broad agreement with our results
126 (Fig. 3f), their modelling implies that dynamic discharge decreased from ~15.5 kyr. Our
127 range of discharge estimates at the LGM (750-2,300 km^3) and in the early Holocene (100-700
128 km^3 at 9 kyr) also fall within their inferred ranges (770-2,750 km^3 and 0-1,650 km^3,
129 respectively). The major difference is that their modelling suggests that dynamic discharge
130 increased from the LGM to a maximum (4,290-4,620 km^3) around the time of Heinrich event
131 1 (H1: 15.5 kyr) when their modelled surface mass balance is largest. A positive mass
132 balance is temporarily induced in the ice sheet modelling[16] shown in Fig. 3f to facilitate a
133 large dynamic discharge from the Hudson Strait Ice Stream during H1. We do not depict such
134 extreme discharge at this time because our approach is based on modern ice stream data that
135 are unlikely to capture such extreme discharges. However, we find no obvious spatial
136 reorganisation[24] of ice streams during or immediately after H1. This suggests that H1 had
137 limited impact on the wider ice sheet drainage network, and points to extreme velocity
138 fluctuations on specific ice streams (e.g. Hudson Strait)[25], which we are unable to constrain,
139 and/or mechanisms that do not invoke major ice sheet collapses and jumps in sea level, such
140 as ice shelf break-up[26]. In contrast, we note some reorganisation of ice streaming following,
141 but not prior to or during, Meltwater Pulse 1A (that began ~14.6 kyr)[27]. The saddle collapse
142 that occurred during separation of the Laurentide and Cordilleran ice sheets has been
143 hypothesised to have contributed to this event[28] and we note several short-lived ice streams in
144 this region after the collapse, but with a concomitant decrease in ice stream activity along the
145 southern margin (Fig. 1c).

146 It is important to consider whether ice streaming in the LIS offers an analogue for
147 modern-day ice sheets. Although the ocean-climate forcing would have been different during
148 deglaciation of the LIS, there is no empirical evidence or theoretical reasoning to suppose
149 that Laurentide ice streams should behave in a fundamentally different manner. Our

reconstructed pattern of ice streams at the LGM is remarkably similar to the velocity pattern of the Greenland and Antarctic Ice Sheets, and we note that Laurentide ice streams drained a similar proportion of the ice sheet perimeter, when it was a similar size to present-day Antarctica (Fig. 1a, b). Large sectors of the LIS occupied similar physiography to modern ice sheets, with ice streams exhibiting a similar size, shape and spatial organisation along its marine margins. The most obvious difference is that the LIS retreated onto a low-relief, hard bedrock terrain and had ice streams that terminated on land and produced large, low-relief lobes along much of the southern and western margins[19,20]. Although these have been likened to some West Antarctic ice streams[19], they have no modern analogue. However, whilst all modern ice streams are marine-terminating, large parts of the Greenland and East Antarctic Ice Sheets will have land-based margins if they continue to deglaciate[29,30], which might be within a few millennia in Greenland[1]. Our analysis confirms that the geology and topography over which modern-ice sheets retreat will be a key determinant on where ice streams are likely to activate and deactivate[8]. However, we also find a strong dependency between ice sheet volume and ice stream activity that also holds for modern ice sheets (Fig. 4c) and which hints at a more regulatory role in ice sheet dynamics than previously recognised. This does not preclude instabilities at decadal to centennial time-scales[5-7], but suggests that if modern ice sheets continue to deglaciate, ice streams are likely to switch off and their relative contribution to mass loss may decrease over several millennia, with final deglaciation accomplished most effectively by surface melt[17,22].

References:

1. Alley, R.B., Clark, P.U., Huybrechts, P. & Joughin, I. Ice-sheet and sea-level changes. *Science* **310**, 456-460 (2005)

2. Rignot, E. & Kanagaratnam, P. Changes in the velocity structure of the Greenland Ice Sheet. *Science* **311**, 986-990 (2006).
3. Rignot, H.D. et al. Recent Antarctic ice mass loss from radar interferometry and regional climate modelling. *Nat. Geosci*. **1**, 106-110 (2008).
4. Rignot, E., Velicogna, I., van den Broeke, M.R., Monaghan, A. & Lenaerts, J.T.M. Acceleration of the contribution of the Greenland and Antarctic ice sheets to sea level rise. *Geophys. Res. Lett*. **38**, L05503 (2011).
5. Golledge, N.R. *et al.* The multi-millennial Antarctic commitment to future sea-level rise. *Nature*, **526**, 421-425 (2015).
6. Feldmann, J. & Levermann, A. Collapse of the West Antarctic Ice Sheet after local destabilization of the Amundsen Basin. *Proc. Nat. Acad. Sci., doi*: 10.1073/pnas.1512482112 (2015).
7. Joughin, I., Smith, B.E. & Medley, B. Marine ice sheet collapse potentially under way for the Thwaites Glacier Basin, West Antarctica. *Science*, **344**, 735-738 (2014).
8. Ritz C. *et al.* Potential sea-level rise from Antarctic ice-sheet instability constrained by observations. *Nature*, doi: 10.1038/nature16147 (2015).
9. IPCC, 2013: Summary for Policymakers. In, Climate Change 2013: The Physical Science Basis. Contribution of Working Group I to the Fifth Assessment Report of the Intergovernmental Panel on Climate Change [Stocker, T.F., Qin, G.-K. Plattner, M. Tignor, S.K. Allen, J. Boschung, A. Nauels, Y. Xia, V. Bex and P.M. Midgley (eds.)]. Cambridge University Press, Cambridge, UK and New York, USA.
10. Kleman, J. & Applegate, P.J. Durations and propagation patterns of ice sheet instability events. *Quat. Sci. Rev*. **92**, 32-29 (2014)
11. Rignot, E. Mouginot, J. & Scheuchl, B, Ice flow of the Antarctic ice sheet. *Science*, **333**, 1427-1430 (2011).

12. Rose, K.E. Characteristics of ice flow in Marie Byrd Land. *J. Glaciol.* **24** (90), 63-75 (1979).
13. Nghiem, S.V. et al. The extreme melt across the Greenland ice sheet in 2012. *Geophys. Res. Lett.* **39**, L20502 (2012)
14. Margold, M., Stokes, C.R., Clark, C.D. & Kleman, J. Ice streams in the Laurentide Ice Sheet: a new mapping inventory. *J. Maps* **11** (3), 380-395 (2015).
15. Dyke, A.S., Moore, A. & Robertson, L. *Deglaciation of North America*. Open File Report, Geological Survey of Canada, Ottawa (2003).
16. Tarasov, L., Dyke, A.S., Neal, R.M. & Peltier, W.R. A data-calibrated distribution of deglacial chronologies for the North American ice complex from glaciological modelling. *Earth and Plan. Sci. Lett*. **315**, 30-40 (2012).
17. Ullman, D.J. et al., Laurentide ice-sheet instability during the last deglaciation. *Nat. Geosci.*, doi: 10.1038/NGEO2463 (2015).
18. Winsborrow, M.C.M., Clark, C.D. & Stokes, C.R. What controls the location of ice streams? *Earth-Sci. Rev*. **103**, 45-59 (2010).
19. Clark, P.U. Surface form of the southern Laurentide Ice Sheet and its implications to ice-sheet dynamics. *Geol. Soc. Am. Bull*. **104**, 595-605 (1992).
20. Ó Cofaigh, C., Evans, D.J.A. and Smith, I.R. Large-scale reorganisation and sedimentation of terrestrial ice streams during late Wisconsinan Laurentide Ice Sheet deglaciation. *Geol. Soc. Am. Bull*. **122** (5-6), 743-756 (2010).
21. Stokes, C.R. & Clark, C.D. Laurentide ice streaming over the Canadian Shield: a conflict with the soft-bedded ice stream paradigm? *Geology* **31** (4), 347-350 (2003).
22. Carlson, A.E. et al. Surface-melt driven Laurentide Ice Sheet retreat during the early Holocene. *Geophys. Res. Lett*. **26** (24), L24502 (2009).

23. Storrar, R.D., Stokes, C.R. & Evans, D.J.A. Increased channelization of subglacial drainage during deglaciation of the Laurentide Ice Sheet. *Geology*, **42** (3), 239-242 (2014).
24. Mooers, H.D. & Lehr, J.D. Terrestrial record of Laurentide Ice Sheet reorganisation during Heinrich events. *Geology* **25** (11), 987 (1997).
25. Hemming, S.R. Heinrich events: massive late Pleistocene detritus layers of the North Atlantic and their global climate imprint. *Revs. Geophys*., **42**, RG1005 (2004).
26. Marcott, S.A. et al. Ice-shelf collapse from subsurface warming as a trigger for Heinrich events. *Proc. Nat. Acad. Sci*. 108 (33), 13415-13419 (2011).
27. Deschamps, P. et al. Ice-sheet collapse and sea-level rise at the Bolling warming 14,600 years ago. *Nature* **483** (7391), 559-564 (2012).
28. Gregoire, L., Payne, A.J. & Valdes, P.J. Deglacial rapid sea level rises caused by ice-sheet saddle collapses. *Nature* **487**, 219-222 (2012).
29. Bamber, J.L. et al. A new bed elevation dataset for Greenland. *The Cryosphere* **7**, 499-510 (2013).
30. Fretwell, P. et al. Bedmap 2: improved ice bed, surface and thickness datasets for Antarctica. *The Cryosphere* **7**, 373-393 (2013).

Supplementary Information is available.

Acknowledgements:

This research was funded by a Natural Environment Research Council award NE/J00782X/1 (C.R.S & C.D.C.). Landsat imagery and the GTOPO30 digital elevation model were provided free of charge by the US Geological Survey Earth Resources Observation Science Centre.

Author contributions:

C.R.S. conceived the study and wrote the proposal with C.D.C. M.M. generated the data on the timing of palaeo-ice streams, modern-ice stream discharge, palaeo-ice stream discharge, and produced the Figures and Supplementary Information, with input from C.R.S. and C.D.C. L.T contributed data from numerical modelling. All authors contributed to the analyses and interpretations of the data. C.R.S. wrote the manuscript with input from all authors.

Author information: Reprints and permissions information is available at www.nature.com/reprints. The authors declare no competing financial interests. Readers are welcome to comment on the online version of the paper. Correspondence and requests for materials should be addressed to C.R.S. (c.r.stokes@durham.ac.uk).

Figures:

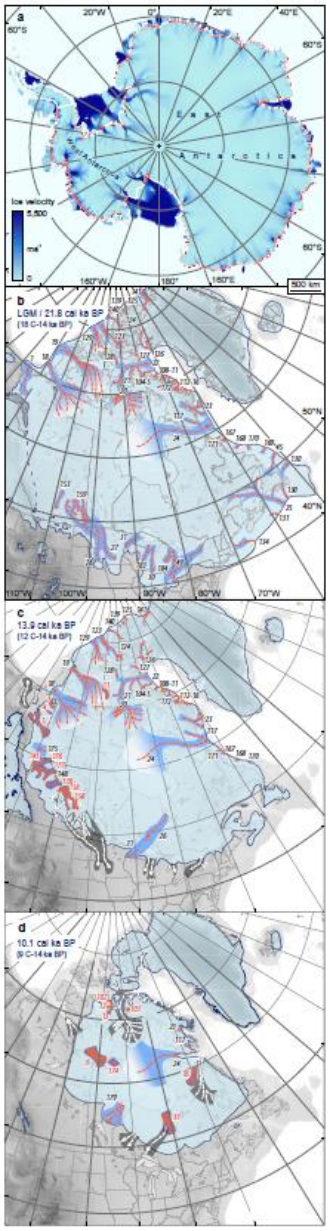

Figure 1: Ice flow velocity of the Antarctic ice sheet[11] compared (at the same scale) with reconstructions of ice stream activity in the LIS at selected time-steps. (**a)** Present-day Antarctic ice sheet velocity[11] with red lines indicating where ice streams intersect the grounding line. Ice streams reconstructed for the LIS at (**b**) the LGM (~21.8 kyr), (**c**) 13.9 kyr, and (**d**) 10.1 kyr. Laurentide ice stream locations in light blue (numbers from the inventory[14]), with those that switched off within the preceding 1,000 years in grey, and those that switched on during the following 1,000 years in dark blue. Underlying topography (**b, c** and **d**) from GTOPO30 digital elevation data.

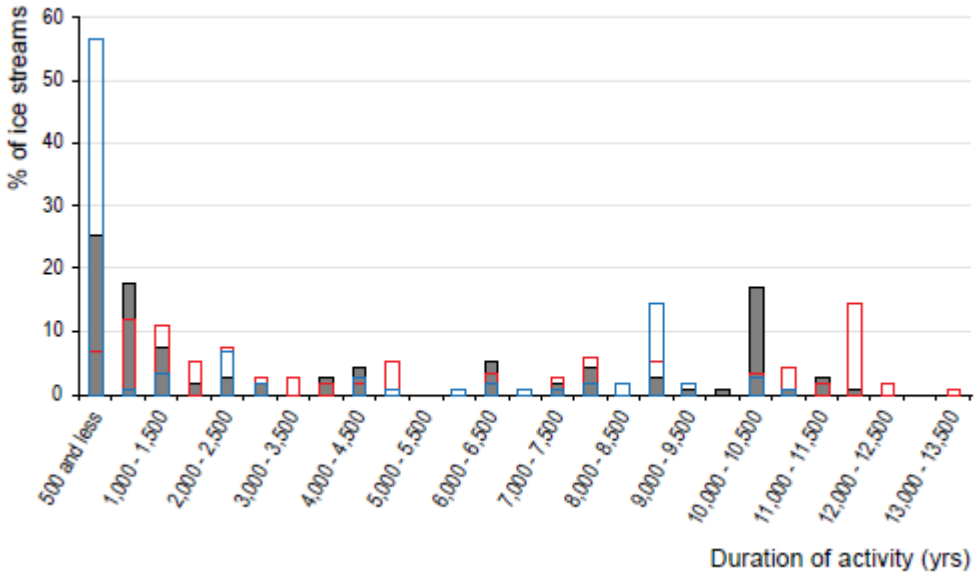

Figure 2: Duration of individual ice streams in the LIS. Grey-filled bars are the data for the best estimate of each ice stream's duration, with blue outlines representing data if the minimum duration is assumed for all ice streams, and red outlines if the maximum duration is assumed for all ice streams (see Extended Data Figure 1 for ice stream locations).

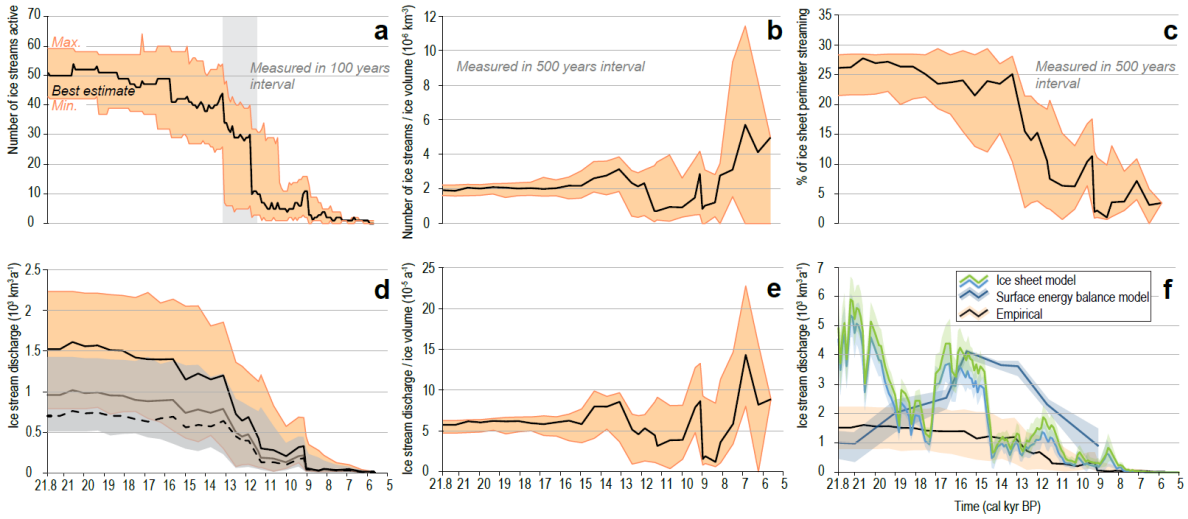

Figure 3: Ice stream activity during deglaciation of the Laurentide Ice Sheet (LIS). (a) Number of ice streams active during deglaciation, with orange shading indicating the uncertainty in the age-bracketing of ice streams and grey vertical bar showing the time when the ice sheet margin transitioned from a predominantly soft to predominantly hard bed. (**b**) Number of active ice streams normalised by LIS volume obtained from a data-calibrated numerical modelling[16]. Orange shading indicates uncertainty in the age-bracketing of ice streams. (**c**) Percentage of the ice sheet perimeter that was streaming, with orange shading indicating uncertainty in the age-bracketing of ice streams. (**d**) First-order estimate of the total ice stream discharge based on a width-discharge regression from modern-ice stream data (see Methods). Orange shading indicates the uncertainty in both the age-bracketing of the ice streams and the discharge uncertainty from the 95% confidence intervals of the regression. For comparison, grey shading shows the range of discharges obtained using the regression without two obvious outliers (Extended Data Figure 10). Dashed line shows discharge from a cruder two state approximation for the best estimate of ice stream duration (see Methods). (**e**) Ice stream discharge (black line in **d**) normalised by LIS volume from numerical modelling[16]. Orange shading indicates the uncertainty in the age-bracketing of ice streams. (**f**) Empirical ice discharge (from **d**) compared to ice stream discharge generated from the mean of a data-calibrated numerical modelling ensemble of the LIS[16]. Light blue line shows streaming discharge from grounded ice-margin grid cells with velocities >500 m a^{-1} and green for grounded margin grid cells >100 m a^{-1} (both with 1-sigma uncertainties). Dark blue shows discharge inferred from previous modelling of the ice sheet's surface mass balance[17].

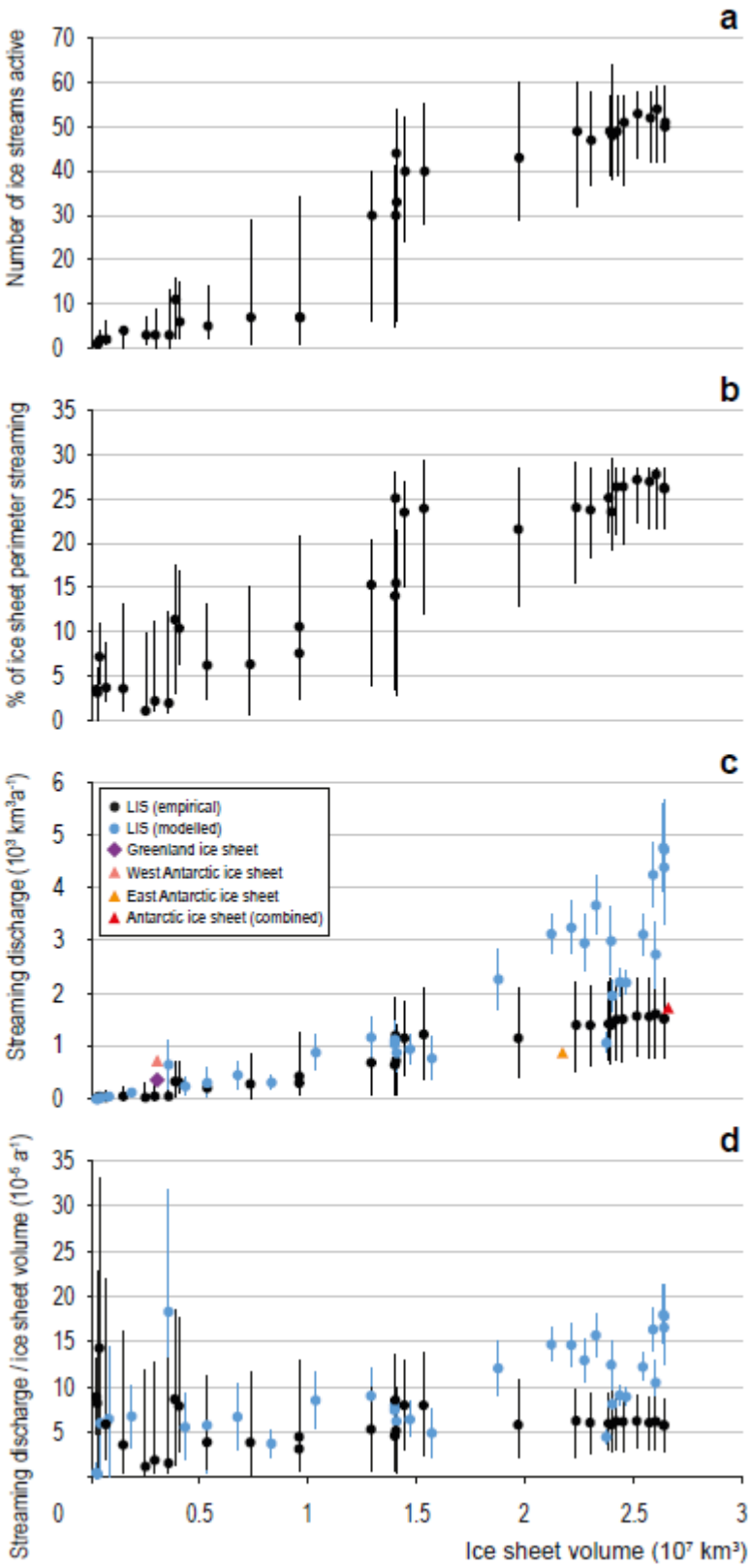

Figure 4: Indicators of ice stream activity plotted against ice sheet volume. (**a**) Number of ice streams plotted against ice sheet volume. Black dots show results using best estimates of ice stream duration with vertical lines showing the uncertainty in the age-bracketing. (**b**)

Percentage of the ice sheet perimeter that was streaming plotted against ice sheet volume (symbols as in (a)). (**c**) Total ice stream discharge plotted against ice sheet volume using our empirical calculations (black dots show best estimate and lines show both the age and discharge uncertainties from Fig. 3d) and total ice stream discharge from numerical modelling[16] (blue dots show mean and lines show 2-sigma uncertainties). Modelled discharge is extracted from grounded ice-marginal grid-cells with velocities >500 m a^{-1} (blue line in Fig. 3f). Data for the present-day ice sheets in Greenland (purple diamond), West Antarctica (pink triangle), East Antarctica (orange triangle) and West and East Antarctica combined (red triangle) are also plotted using recent ice stream discharge[2,3] and ice sheet volume[29,30] estimates. (**d**) Total ice stream discharge from modelled and empirical estimates in (**c**) normalised by ice sheet volume and plotted against ice sheet volume. In all panels, ice sheet volume is derived from the mean of a best-performing ensemble of previously-published data-calibrated numerical modelling[15] (see Methods). Note that the low modelled streaming fraction at volumes around 2.4 x 10^7 km^3 (**c** & **d**) are due to the dynamic facilitation of Heinrich event 1 in that modelling (see Methods). Empirical discharges for small ice volumes (< 0.2 x 10^7 km^3) have highly under-represented uncertainties given higher ice sheet volume uncertainties close to final deglaciation.

METHODS:

Identifying palaeo-ice stream locations: An ice stream is a region in a grounded ice sheet that flows much faster than the regions on either side[31]. Where the fast-flowing ice becomes bordered by exposed rock (e.g. in high relief fjord landscapes) they are usually referred to as marine-terminating outlet glaciers. These outlet glaciers typically initiate as ice streams and so we use the term 'ice stream' throughout, but include outlet glaciers.

We use a recently-published inventory[14] of palaeo-ice streams in the Laurentide Ice Sheet (LIS), which includes 117 ice streams (Extended Data Figure 1). These were identified based on previously published evidence, complemented with new mapping using satellite imagery and Digital Elevation Models (DEMs) on land, and bathymetric data and swath bathymetry for submerged areas[14]. The systematic nature of the new mapping from across the entire ice sheet bed means it is very unlikely that any major ice streams have been missed[14].

Ice streams are easily distinguishable on a palaeo-ice sheet bed from a variety of evidence that is now well-established in the literature[14,20,21,32-43]. Their spatially discrete enhanced flow creates a distinctive bedform imprint that is immediately recognisable and characterised by several geomorphological criteria[32]. These include highly elongated subglacial bedforms (mega-scale glacial lineations[34]: Extended Data Figures 4 & 5), which have also been observed beneath modern ice streams[35], and these bedforms typically exhibit convergent flow patterns towards a main ice stream 'trunk'. These landform assemblages are often characterised by abrupt lateral margins that border areas with much shorter subglacial bedforms, or no bedforms at all[32,33,36,37,42,43] (Extended Data Figure 5). In some cases, the abrupt margin is marked by features known as ice stream shear margin moraines[32,33,37,38] (Extended Data Figure 5). This landform evidence is readily identifiable on satellite imagery and aerial photographs[32,34,36-39,43] and, in some cases, is further augmented by field investigations that reveal discrete (Boothia-type)[33] erratic dispersal trains or sedimentological evidence from tills that may have been overridden and/or deformed by rapid ice flow. However, there are no ice streams in the inventory that are based only on sedimentological data and most (>85%) have a clear bedform imprint[14].

At a larger spatial scale, it is known that many ice streams are steered by the underlying topography, often forming marine-terminating outlet glaciers bordered by rock walls[2-4]. The inventory includes these topographic ice streams, many of which were identified by major cross shelf-troughs and their associated sedimentary depocentres[40] (Extended Data Figure 6). Swath bathymetry from within these troughs commonly reveals many of the geomorphological criteria[32] described above, such as mega-scale glacial lineations[34,35,42].

Given previous work that highlights the importance of 'soft' bedrock geology in influencing ice stream location[10,18,19], we also analysed the type of bedrock over which each ice stream was located. We categorized their underlying geology as either (i) predominantly 'soft' sedimentary rocks, (ii) predominantly 'hard' crystalline rocks (intrusive, metamorphic and volcanic rocks) or (iii) those where the spatial footprint of the ice stream extended over a mixture of both soft and hard rocks. This allowed us to calculate the number of different types of ice streams on each broad geological category through time (Extended Data Figure 3).

Dating palaeo-ice streams: We used the best-available pan-ice sheet margin chronology[15] to bracket the age of the spatial footprints of each ice stream in the inventory[14]. The ice margin chronology includes 32 time-steps, starting at 21.8 kyr (18 14C yr), ending at 5.7 kyr (5 14C yr), and based on >4,000 dates that are spread across the entire ice sheet bed (Extended Data Figure 2). The database consists of mainly radiocarbon dates, supplemented with varve and tephra dates, which constrain ice margin positions, and shorelines of large glacial lakes. Dates on problematic materials (e.g. marl, freshwater shells, lake sediment with low organic carbon content, marine sediment, bulk samples with probable blended ages, and most deposit feeding molluscs from calcareous substrates) were excluded. Marine shell dates, a major component, were adjusted for regionally variable marine reservoir effects based on a large new set of radiocarbon ages on live-collected, pre-bomb molluscs from Pacific, Arctic, and Atlantic shores. We use a mixed marine and Northern Hemisphere atmosphere calibration curve while Dyke et al.[15] used IntCal98 calibration curve.

We used the ice margin chronology to bracket the duration of ice stream activity using methods employed in previous work on individual or small numbers of ice streams[21,36,41-43] (Extended Data Figure 7). In some cases, the duration of ice streaming may have been short-lived (just few hundred years), leaving evidence of a simple 'rubber-stamped' imprint[32] of their activity, the spatial extent of which can be readily matched to just one or two ice margin positions (Extended Data Figure 7a). The more complex landform assemblages of other ice streams (with overprinted MSGLs linked to associated ice marginal features) clearly indicate that they continued to operate during ice margin retreat (Extended Data Figure 7b), and we therefore fit the ice stream activity to a series of ice margin positions over a longer-timespan (hundreds to thousands of years). Similar patterns are seen for marine-terminating ice streams[42] (Extended Data Figure 7c and 7d).

To account for the inherent uncertainties in the dating (and interpolated ice margin position) and the spatial extent of each ice stream, we provide a maximum possible duration and a minimum duration for each ice stream in the inventory (Figure 2). It should be noted that in some cases where the interpolated ice margin positions indicated a very short duration of ice streaming, we set the minimum duration to 100 years. This is because the creation of subglacial bedforms that permits their identification is likely to be of the order of decades[35] and attempting to date to a higher precision is meaningless given the dating uncertainties (mainly radiocarbon) and our focus on millennial-scale changes throughout deglaciation.

Estimating palaeo-ice stream discharges: Unfortunately, there is no direct means to empirically reconstruct the velocity, and thus discharge, of a palaeo-ice stream from the evidence it left behind. In order to provide a simple, first-order estimate of the potential ice discharge from each palaeo-ice stream where only the width is known confidently, we used an empirical relationship between the with and discharge of 81 active ice streams in Antarctica (50: Extended Data Figure 8) and Greenland (31: Extended Data Figure 9). Ice velocities (m a^{-1}) were extracted from recent compilations in Greenland (2008-2009)[44] and Antarctica (2007-2009)[45] and we used these velocity datasets to measure the width (km) of

the ice stream (to the lateral shear margins or exposed rock walls) at the grounding line[29,45]. Velocity was extracted as a width-averaged value. We then used the highest resolution bed-data that was available for Greenland[29] and Antarctica[30] to calculate the cross-sectional area (km^2) of each ice stream at the grounding line. We then calculated the modern ice stream discharge ($km^3\ a^{-1}$) by multiplying the velocity data by the ice-thickness data and integrating the output along the ice stream's width at the grounding line.

When ice stream data from Antarctica and Greenland are amalgamated (Extended Data Figure 10), a simple linear regression reveals a weak correlation ($R^2 = 0.39$) between their width and discharge, which we use to predict an order-of-magnitude palaeo-discharge from the width of each palaeo-ice stream that was active during deglaciation at each dated margin position (Figure 3d). The regression is clearly influenced by two outliers with extremely high discharge (Pine Island Glacier and Thwaites Glacier, West Antarctica). Without them, the correlation weakens ($R^2 = 0.31$) and our palaeo-discharge estimates show the same trend, but absolute discharges are lower (see grey shading on Fig. 3d). We considered removing them from the regression, but use them in our estimates of palaeo-discharge (e.g. in Fig. 3e and f, and Fig. 4c and d) because they allow us to partly capture some of the more extreme discharges that might be expected in a deglaciating ice sheet. We also extract the 95% confidence intervals of the regression and use these to estimate a lower and upper range of discharge for an ice stream of given width. It should be noted, however, that these confidence intervals under-represent the uncertainty because some assumptions for those confidence intervals (and the general validity of linear regression) are broken: a) Gaussian noise, b) no correlation between individual data point residuals, c) constant variance. Given this, and the obvious (and perhaps not surprising) complexity of the relationship between discharge and width for modern ice streams (e.g. the mean value of linear ice stream flux for Greenlandic ice streams is very different from that for Antarctic ice streams, where there is a stronger relationship), we also extract a discharge relationship with a cruder two state approximation that avoids the assumptions required for statistically robust application of linear regression. It is also important to note that the modern ice stream data are from one short time-period and yet we know that ice streams with a fixed width can accelerate (and decelerate) at short (annual-decadal) time-scales[2-4]. However, the extent to which these accelerations and decelerations are sustained over longer (centennial-millennial) time-scales is presently unknown. Thus, we use this simple approach to generate the first empirical order-of-magnitude estimate of palaeo-discharge from the LIS averaged over millennial time-scales and note that our empirical results are broadly similar to those generated by numerical modelling[16,17] (Fig. 3f), albeit typically lower.

To evaluate our empirical estimates of palaeo-ice stream discharge in relation to ice sheet volume (e.g. Fig's 3d, 3e and Fig. 4), we extracted ice sheet volume from the mean of an ensemble of best-performing model runs from a previously-published data-calibrated numerical model[16]. Uncertainties associated with the modelled ice volumes (see Ref. 15) are an order of magnitude less than those associated with our estimates of palaeo-ice stream discharge and are not shown (e.g. in Fig. 4). We use this same model to compare our empirical estimates of ice stream discharge against those generated in a numerical model of

the LIS, with streaming discharge extracted from an ensemble of best-performing model runs at 100 year time-steps during deglaciation from 21.8 to 5.7 kyr, and ensemble standard deviation in ice stream discharge shown in shading around the mean (Fig. 3f). The weighted ensemble mean from this model shows a similar trend of decreasing discharge from ice streams (Fig. 3f), but with higher discharges and greater variability. This is to be expected because our estimates based on modern ice stream discharges may not capture the full range of ice stream behaviour during deglaciation of a mid-latitude ice sheet (e.g., we have no modern analogue of an extensive land-terminating margin overlying soft sediments). It should also be noted that the numerical modelling imposes a data-calibrated reduction in ice streaming around the Hudson Strait region just prior to Heinrich event 1 in order to facilitate a dynamic destabilisation during H1. This is reflected in the reduced streaming discharge in that model for a few thousand years prior to 17 ka and a temporary increase thereafter (Fig. 3f and Fig. 4c and d). It is also reflected in the low modelled streaming fraction at volumes around 2.4 x 10^7 km^3 (see Fig. 4d).

Methods References

31. Patterson, W.S.B. *The Physics of Glaciers* (3rd Ed). Pergamon, UK (1994).
32. Stokes, C.R. & Clark, C.D. Geomorphological criteria for identifying Pleistocene ice streams. *A. Glac*. **28**, 67-75 (1999).
33. Dyke, A.S. & Morris, T.F. Canadian landform examples. 7. Drumlin fields, dispersal trains, and ice streams in Arctic Canada. *Can. Geogr*. **32** (1), 86-90 (1988).
34. Clark, C.D. Mega-scale glacial lineations and cross-cutting ice flow landforms. *Earth Surf. Proc. Land.* **18** (1), 1-29 (1993).
35. King, E.C. Hindmarsh, R.C.A. & Stokes, C.R. Formation of mega-scale glacial lineations observed beneath a West Antarctic ice stream. *Nat. Geosci.* **2** (8), 585-588 (2009).
36. Clark, C.D. & Stokes, C.R. Extent and basal characteristics of the M'Clintock Channel Ice Stream. *Quat. Int.* **86** (1), 81-101 (2001).
37. Hodgson, D.A. Episodic ice streams and ice shelves during retreat of the northwesternmost sector of the late Wisconsinan Laurentide Ice Sheet over the central Canadian Arctic Archipelago. *Boreas* **23** (1), 14-28 (1994).
38. Stokes, C.R. & Clark, C.D. Ice stream shear margin moraines. *Earth Surf. Proc. Land.* **27** (5), 547-558 (2002)
39. Stokes, C.R. Identification and mapping of palaeo-ice stream geomorphology from satellite imagery: implications for ice stream functioning and ice sheet dynamics. *Int. J. Remote Sens.* **23** (8), 1557-1563 (2002).
40. Batchelor, C.L. & Dowdeswell, J.A. The physiography of high Arctic cross-shelf troughs. *Quat. Sci. Rev.* **92**, 68-96 (2014).
41. Stokes, C.R. & Clark, C.D. Palaeo-ice streams. *Quat. Sci. Rev*. **20** (13), 1437-1457 (2001).
42. O'Cofaigh, C., Dowdeswell, J.A., Evans, J. & Larter, R.D. Geological constraints on Antarctic palaeo-ice stream retreat. *Earth. Surf. Proc. Land*. **33** (4), 513-525 (2008).

43. Stokes, C.R., Clark, C.D. & Storrar, R.D. Major changes in ice stream dynamics during deglaciation of the north-western margin of the Laurentide Ice Sheet. *Quat. Sci. Rev*. **28** (7), 721-738 (2009).
44. Joughin, I., Smith, B., Howat, I. & Scambos, T. MEaSUREs Greenland Ice Sheet Velocity Map from InSAR Data. National Snow and Ice Data Center, Boulder, Colorado USA (2010).
45. Rignot, E., Mouginot, J. & Scheuchl, B. MEaSUREs InSAR-Based Antarctica Ice Velocity Map. National Snow and Ice Data Center, Boulder, Colorado USA (2011).
46. Rignot, E., Mouginot, J. & Scheuchl, B. Antarctic grounding line mapping from differential satellite radar interferometry. *Geophys. Res. Lett*., **38** (10): L10504 (2011).

Extended Data Figure Legends:

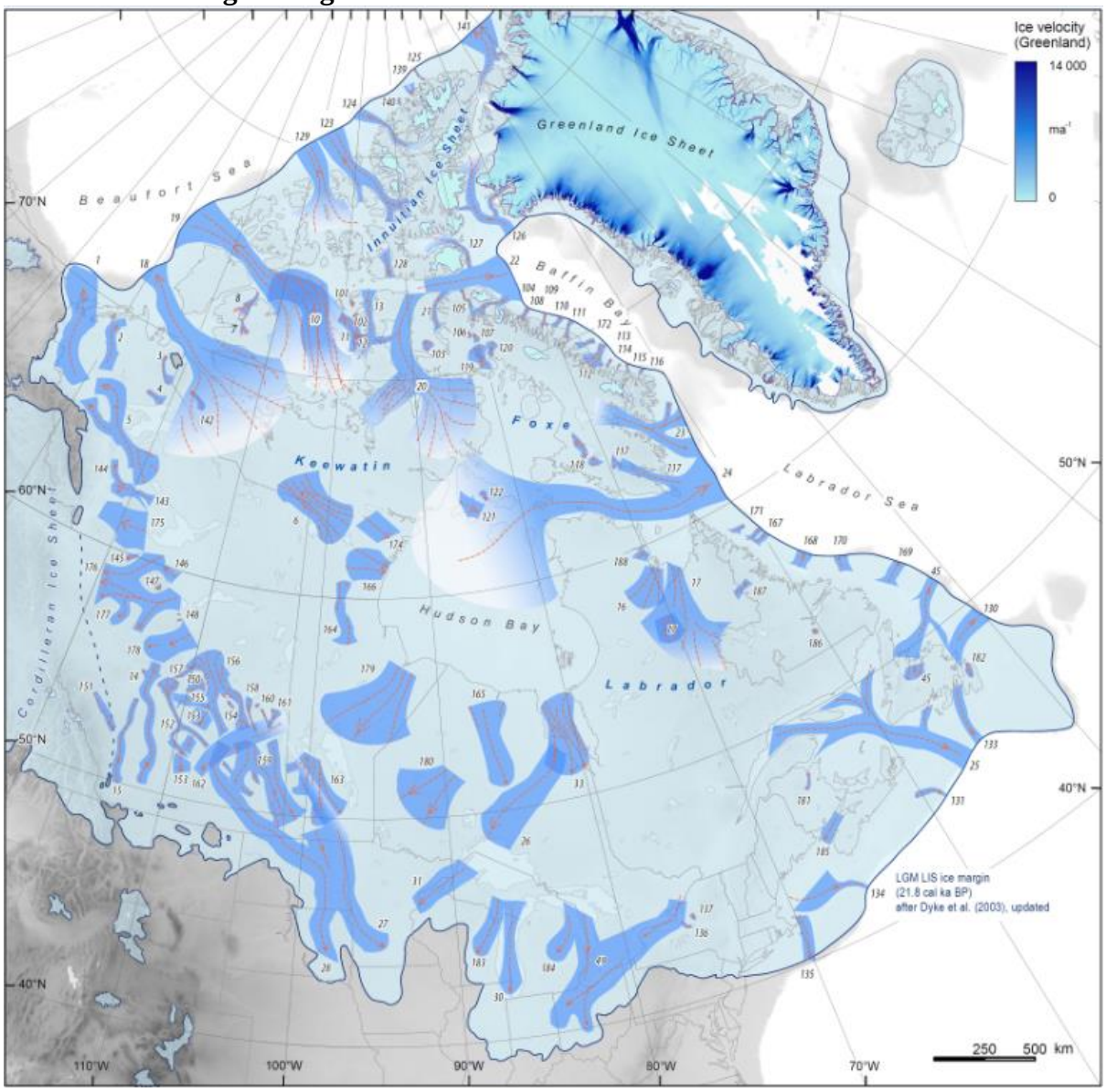

Extended Data Figure 1: Location of 117 ice streams from a recently-compiled inventory[14] based on previous work and systematic mapping across the ice sheet bed. Palaeo-ice streams are shown in dark blue shading and numbered as in ref. 14. Modern-day ice velocity is shown for Greenland[44]. Underlying topography from GTOPO30 digital elevation data[47].

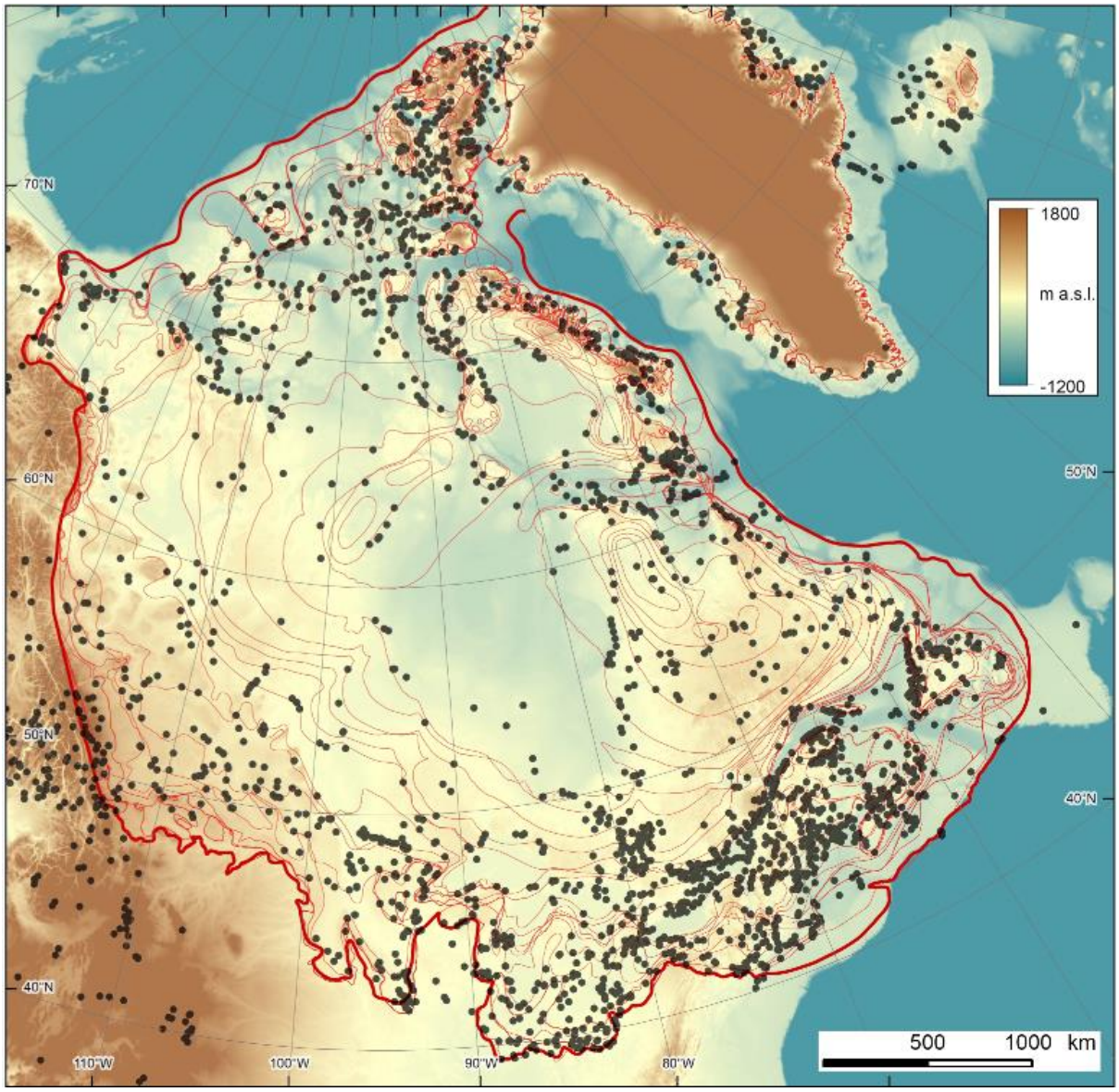

Extended Data Figure 2: Distribution of dates and interpolated ice margin positions from Dyke et al. (2003)[14]. These ice margin positions (thin red lines) are based on dates (black dots) that we used to bracket the age of the spatial footprint of each ice stream (Extended Data Figure 7). The thick red line shows the updated LGM ice margin (following recent work[49-55]). Underlying topography from GTOPO30 digital elevation data [47].

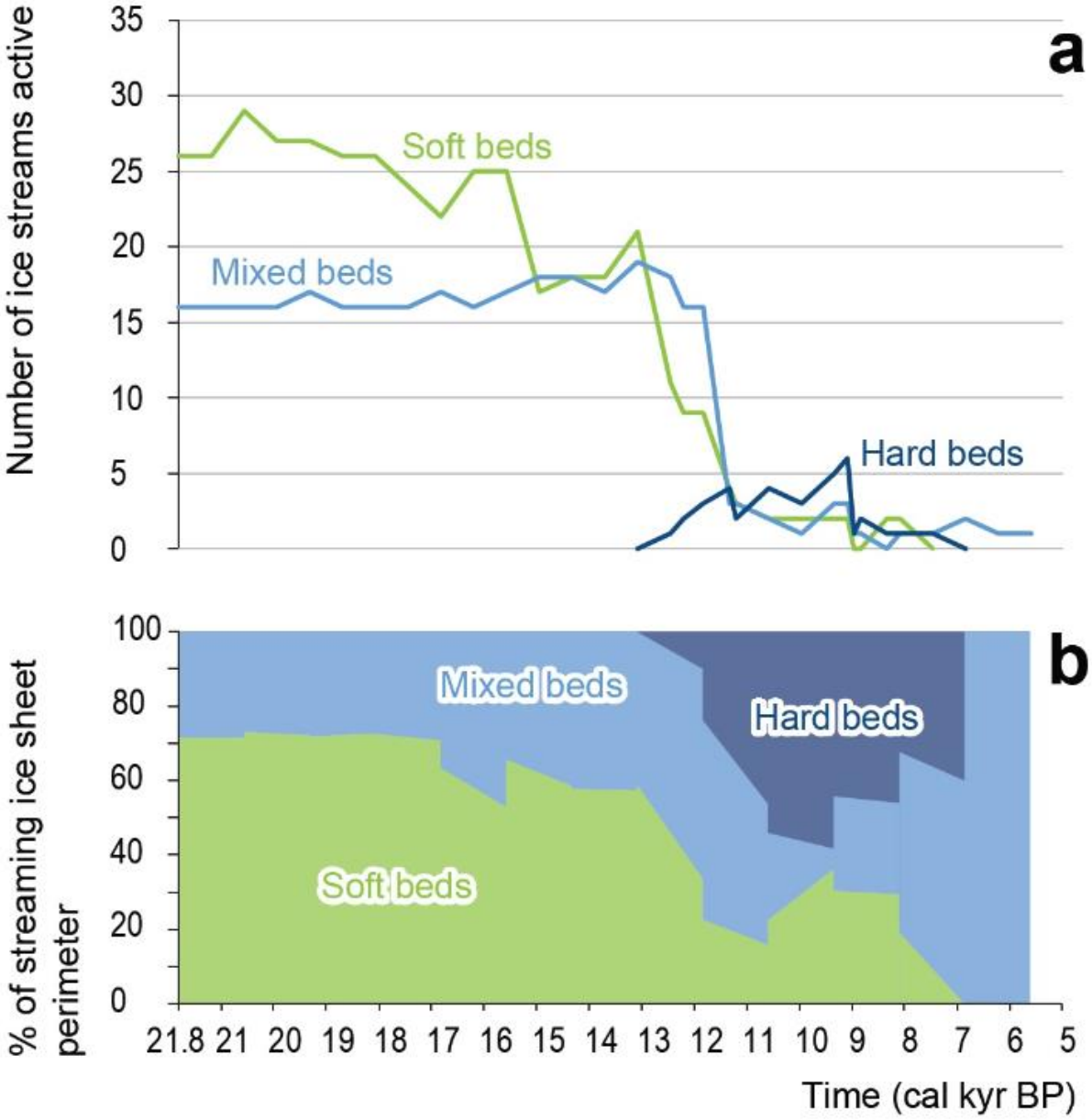

517

518 **Extended Data Figure 3: The number of ice streams and the percentage of the margin**
519 **they drained through time, classified according to their underlying geology. (a)** A sharp
520 drop in the number of ice streams is observed after ~12 kyr (Fig. 3a) which is linked with the
521 retreat onto the hard crystalline rocks of the Canadian Shield[19]. (**b**) Note, however, that
522 several large, wide ice streams were active over the hard bed geology (e.g. refs. 10, 21) and
523 they drained a large percentage of the ice sheet's perimeter.

524

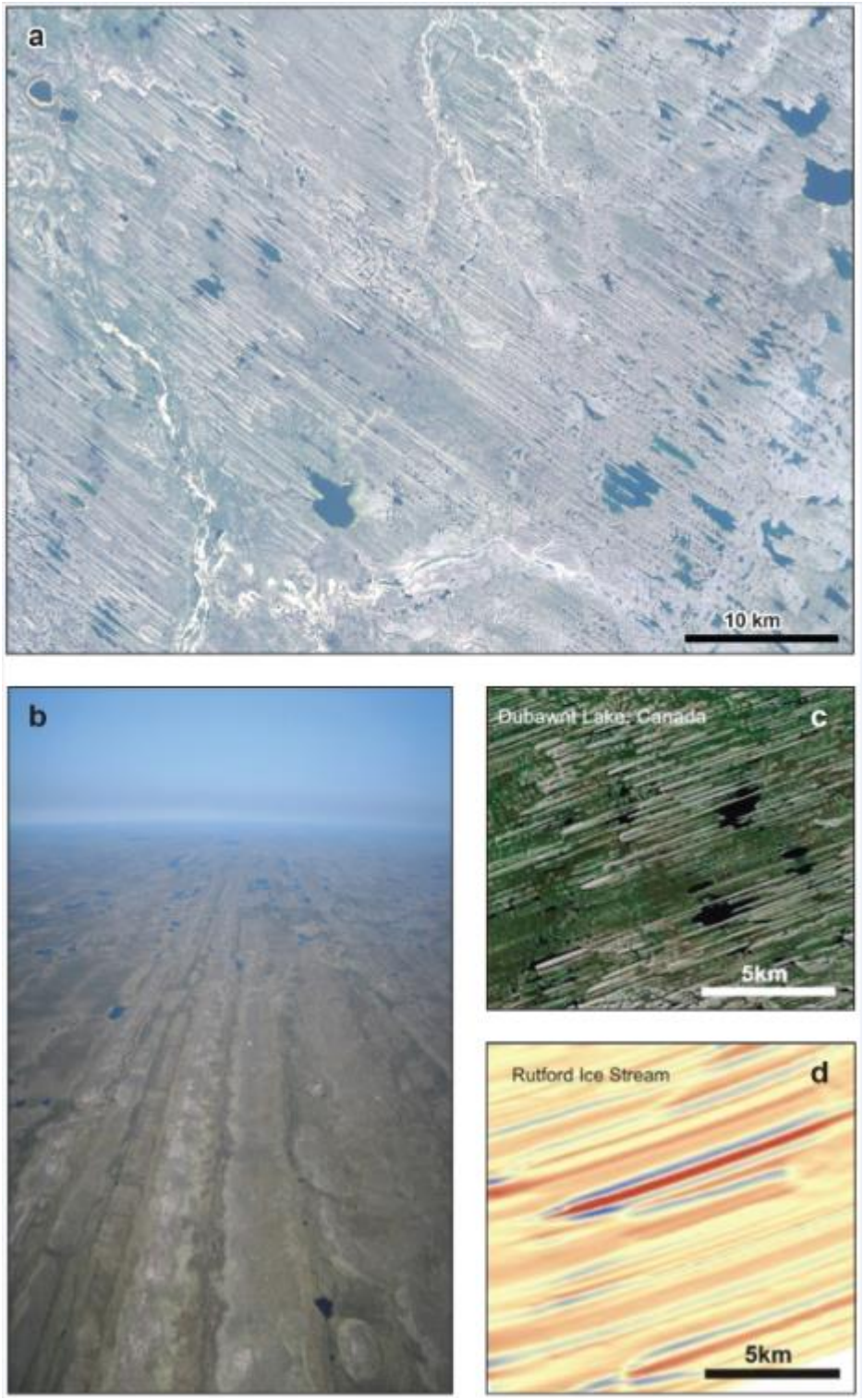

Extended Data Figure 4: Mega-scale glacial lineations[34] on the Dubawnt Lake Ice Stream bed[21], central Canada. These features are a characteristic geomorphological signature of ice streaming and are readily identifiable on Landsat satellite imagery (**a** and **c**) and oblique aerial photography (**b**) of the ice stream bed (no. 6 on Extended Data Figure 1). Identical features have been detected beneath Rutford Ice Stream in West Antarctica[35] in (d). Landsat imagery courtesy of the US Geological Survey Earth Resources Observation Science Centre and photograph by Chris Stokes. Images in (**c**) and (**d**) modified from ref. 35.

533

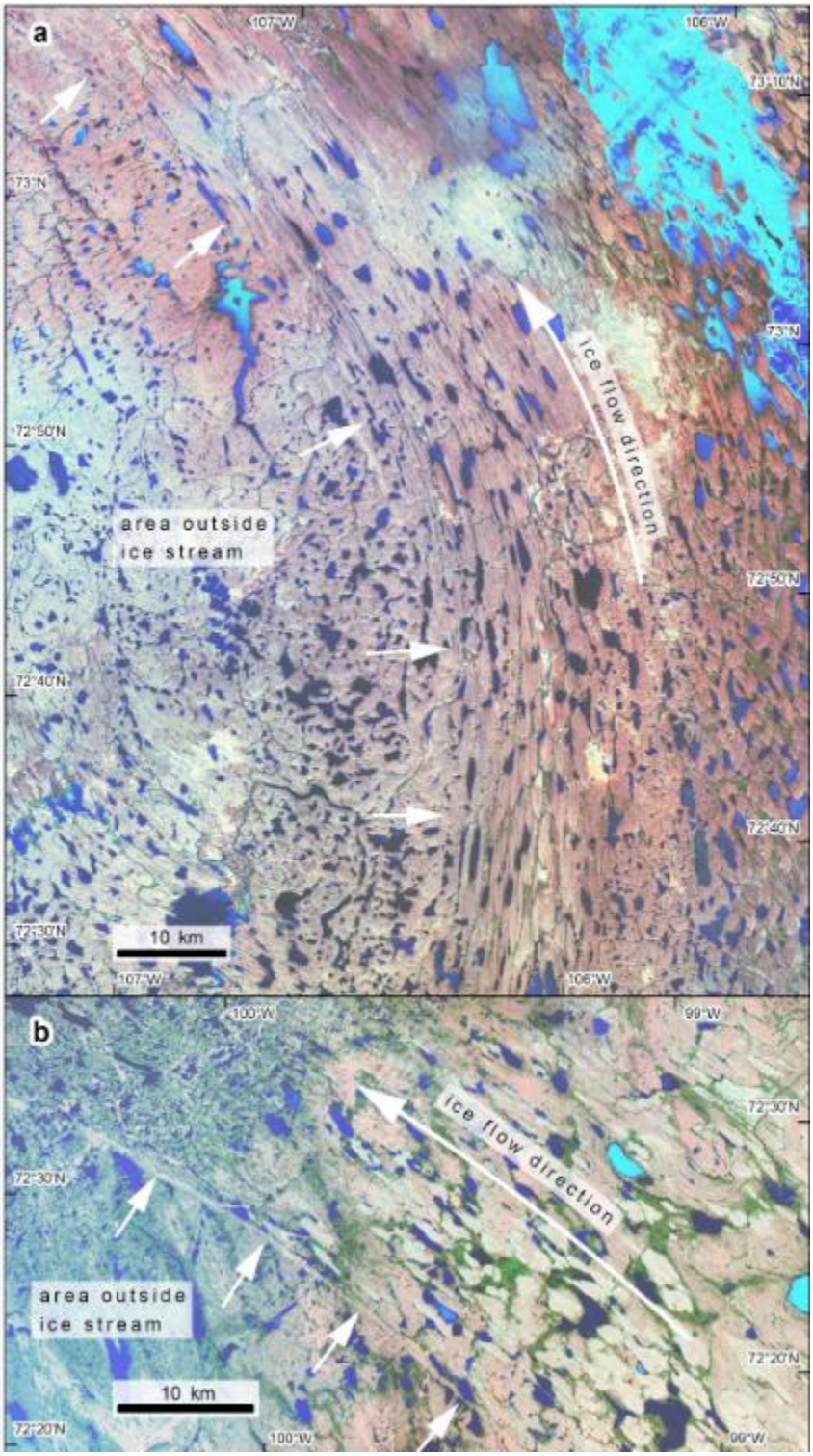

Extended Data Figure 5: Landsat imagery of lateral shear margin moraines in the Canadian Arctic Archipelago. (**a**) The M'Clintock Channel Ice Stream bed[36,37] on Victoria Island (no. 10 on Extended Data Fig. 1), and (**b**) the Crooked Lake Ice Stream[33] on Prince of Wales Island (no 11 on Extended Data Fig. 1). Note the abrupt lateral margins (marked by white arrows) of the assemblage of mega-scale glacial lineations that is, in places, marked by lateral shear margin moraines[38].

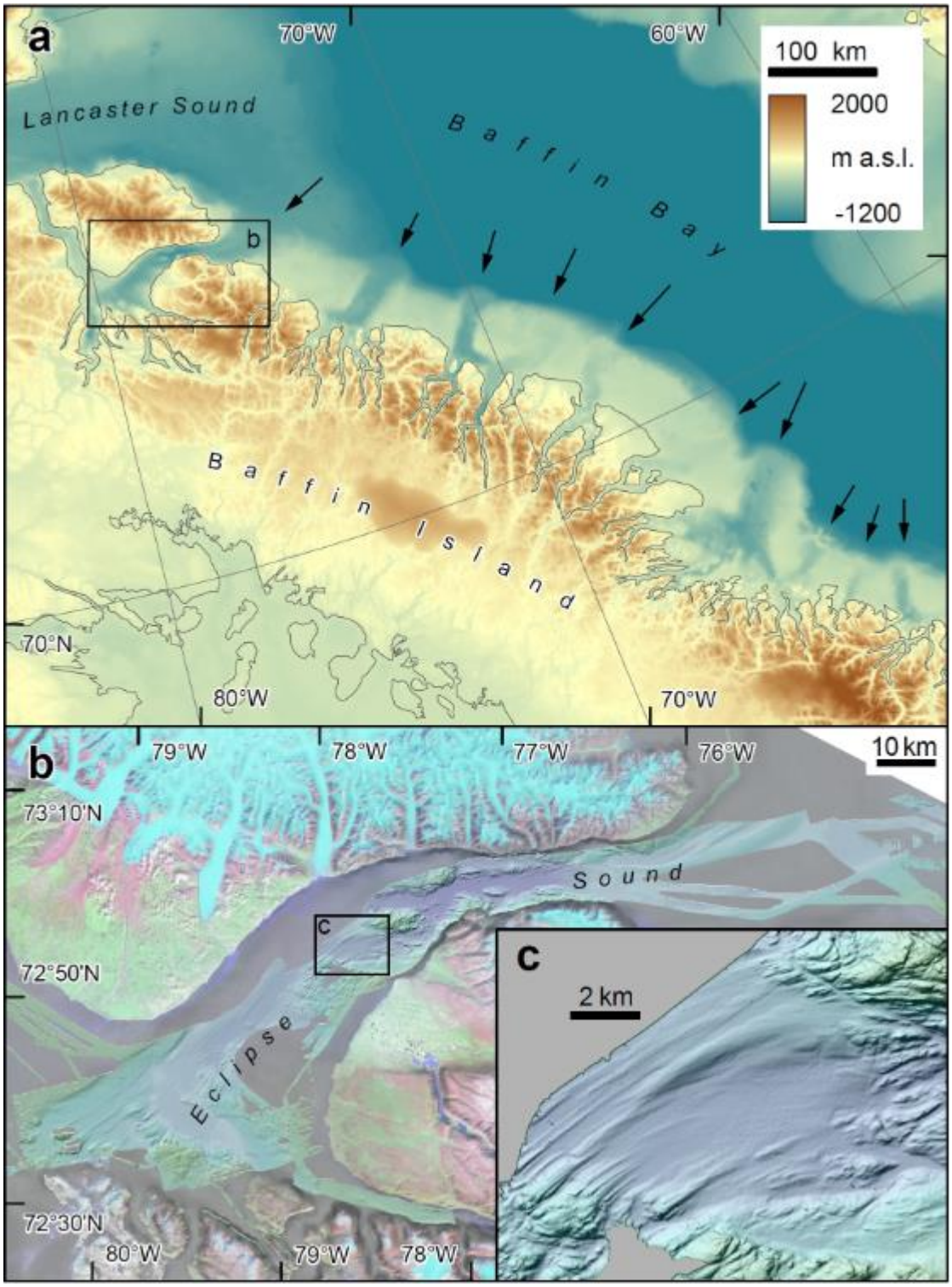

Extended Data Figure 6: Bathymetric data showing cross-shelf troughs and a well-preserved bedform imprint from a submarine setting. (**a**) Cross-shelf troughs formed by ice streams fed by convergence of ice flow from several fjords along the east coast of Baffin Island. (**b**) Drumlins and mega-scale glacial lineations on the floor of Eclipse Sound (location shown in (**a**)). High resolution swath bathymetry data in (**a**) from IBCAO[56] and in (**b** and **c**) from IBCAO[56] and ArcticNet[57]. Figure redrawn from Margold et al. (2015)[48].

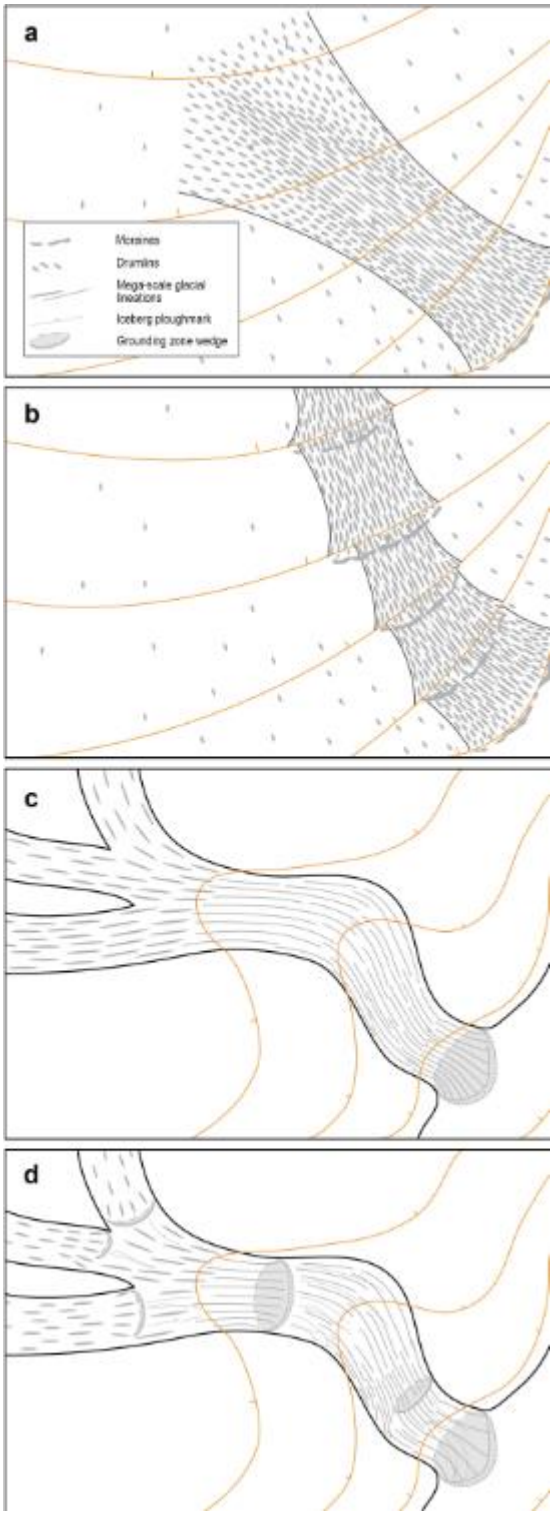

Extended Data Figure 7: Schematic demonstrating the method used to bracket the age of the spatial footprint of palaeo-ice streams in both terrestrial and marine settings. These methods have been used extensively in previous work, but usually on small samples of ice streams (e.g. refs [20,21, 36, 37, 42,43]). In some cases, terrestrial ice streams are active, but then deactivate (shutdown) as the ice margin retreats (**a**), enabling them to be bracketed between a small number of dated ice margins and implying a short duration of operation. In other cases, ice streams remain active during deglaciation and continually remould their landform

assemblage, leaving a more complicated time-integrated landform record, often with a series of overprinted landforms (**b**), and implying a longer duration of operation. The same scenarios are shown for a topographically-controlled marine-terminating ice stream in (**c**) and (**d**).

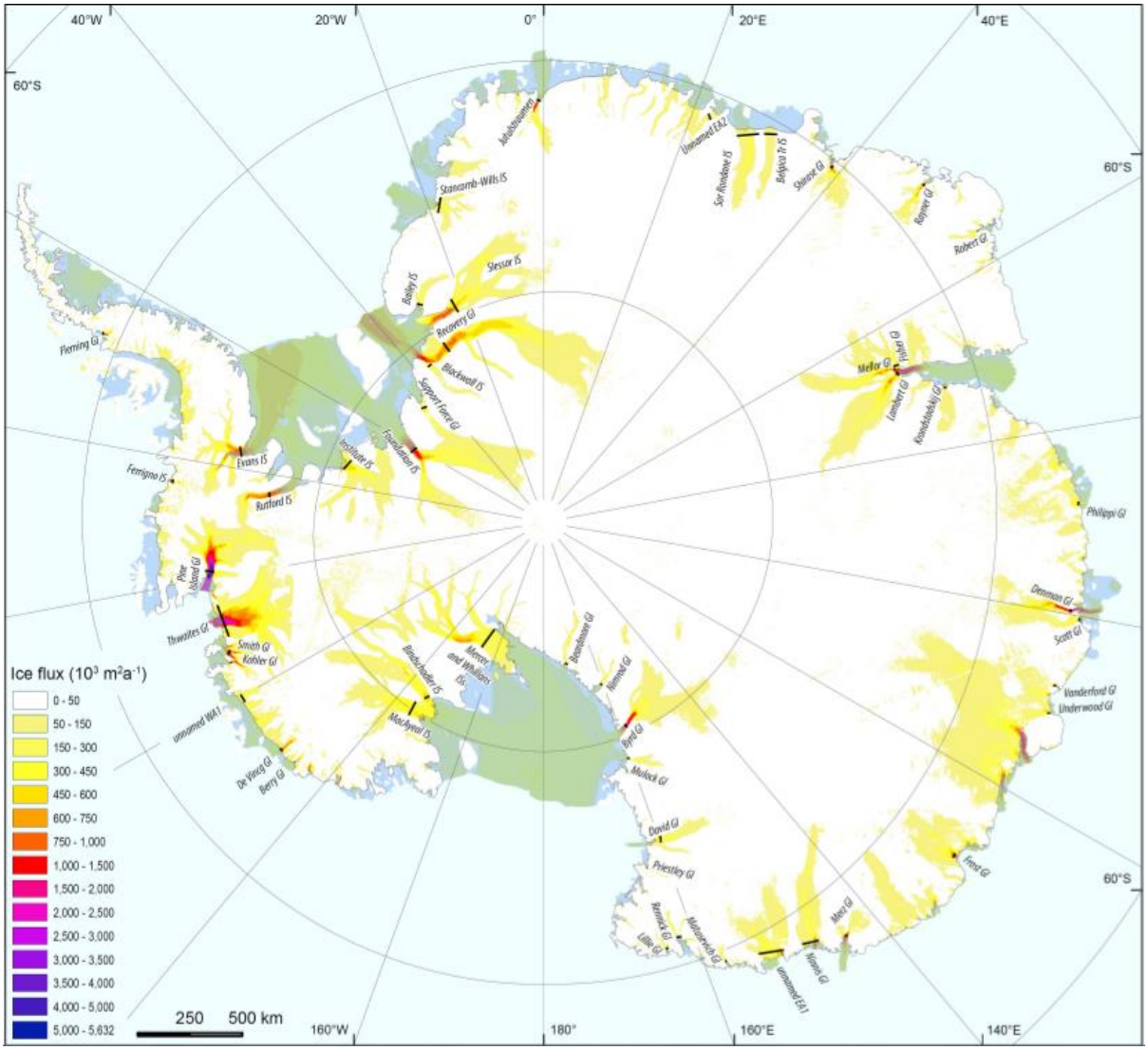

Extended Data Figure 8: Location of ice streams in Antarctica where discharge was estimated from existing datasets of velocity[45], grounding line position[46] and ice thickness[30]. Regression analysis reveals a weak relationship between their width and discharge (Extended Data Figure 10), which we use to estimate the discharge of palaeo-ice streams where we only know their width (see Methods)

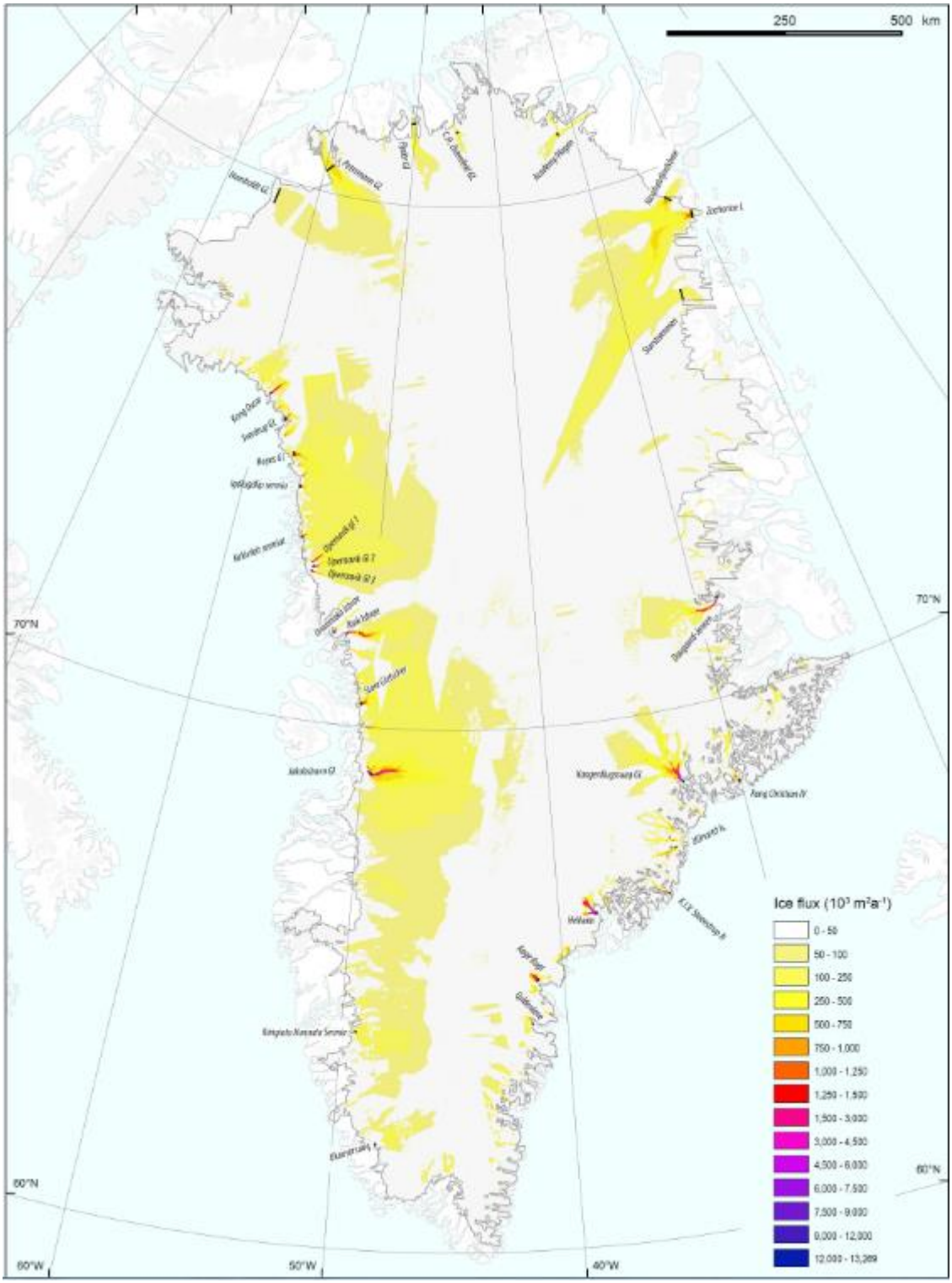

Extended Data Figure 9: Location of ice streams in Greenland where discharge was estimated from existing datasets of velocity[44], grounding line position[44] and ice thickness[29]. Regression analysis reveals a weak relationship between their width and discharge (Extended Data Figure 10), which we use to estimate the discharge of palaeo-ice streams where we only know their width (see Methods)

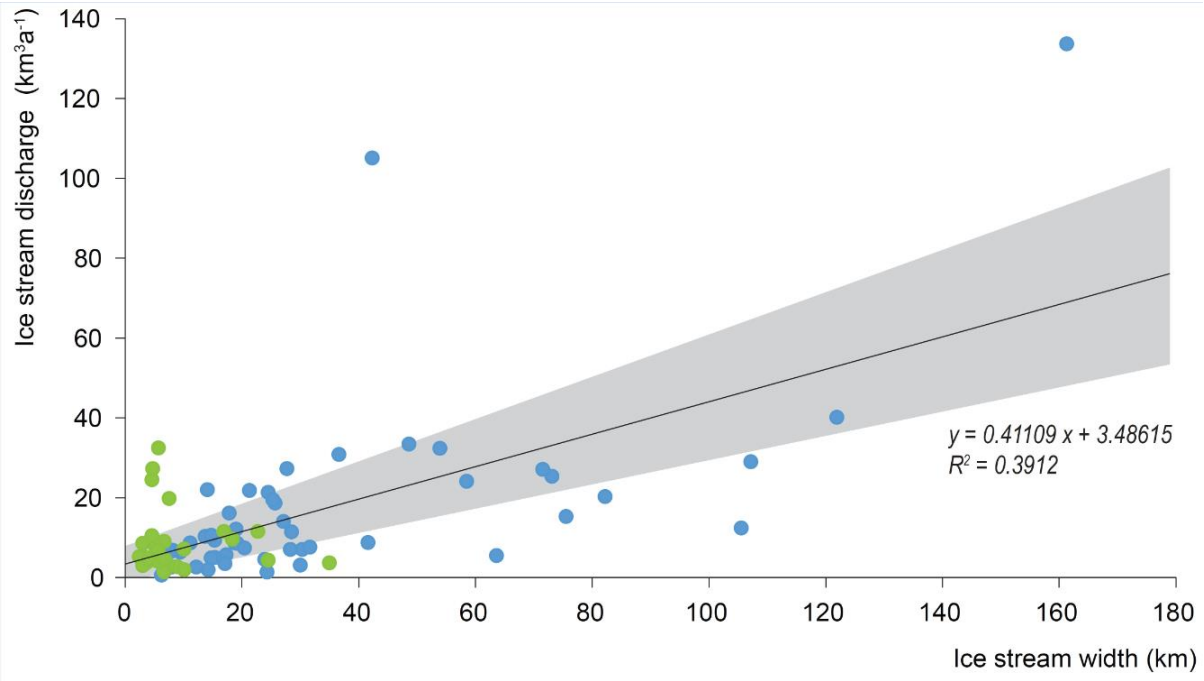

Extended Data Figure 10: Relationship between ice stream discharge and width for 81 active ice streams in Antarctica and Greenland. Discharge calculations derived from velocity data in 2008-2009 (Greenland: green dots)[44] and 2007-2009 (Antarctica: blue dots)[46]. Grey shading shows the 95% confidence intervals of the linear regression. Measured ice stream locations are shown in Extended Data Figure's 8 and 9.

Extended Data References:

47. Global Digital Elevation Model (GTOPO30), U.S. Geological Survey, EROS Data Center Distributed Active Archive Center (EDC DAAC). Edition 2004.
48. Margold, M., Stokes, C.R. & Clark, C.D. Ice streams in the Laurentide Ice Sheet: identification, characteristics and comparison to modern ice sheets. *Earth-Science Reviews* **143**, 117-146 (2015).
49. Briner, J.P., Miller, G.H., Davis, P.T. & Finkel, R.C. Cosmogenic radionuclides from fjord landscapes support differential erosion by overriding ice sheets. *Geol. Soc. Am. Bull.* **118** (3-4), 406-420 (2006).
50. Shaw, J. et al., A conceptual model of the deglaciation of Atlantic Canada. *Quat. Sci. Rev.* **19** (10), 959-980 (2006).
51. Kleman, J. et al., North American Ice Sheet build-up during the last glacial cycle, 115-21 kyr. *Quat. Sci. Rev.* **29** (17-18), 2036-2051 (2010).
52. Lakeman, T.R., & England, J.H. Palaeo-glaciological insights from the age and morphology of the Jesse moraine belt, western Canadian Arctic. *Quat. Sci. Rev.* **47**, 82-100 (2012).
53. Lakeman, T.R., & England, J.H. Late Wisconsinan glaciation and postglacial relative sea-level change on western Banks Island, Canadian Arctic Archipelago. *Quat. Sci. Rev.* **80** (1), 99-112 (2013).
54. Jakobsson, M. et al., Arctic Ocean glacial history. *Quat. Sci. Rev.* **92**, 40-67 (2014).

55. Nixon, F.C. & England. J.H. Expanded Late Wisconsinan ice cap and ice sheet margins in the western Queen Elizabeth Islands, Arctic Canada. *Quat. Sci. Rev*. **91**, 146-164 (2014).
56. Jakobsson, M. et al., The International Bathymetric Chart of the Arctic Ocean (IBCAO) Version 3.0. *Geophys. Res. Lett*., doi: 10.1029/2012GL052219 (2012).
57. ArcticNet, 2013: http://www.omg.unb.ca/Projects/Arctic/ [accessed 1st December 2013]